

NOTICE WARNING CONCERNING COPYRIGHT RESTRICTIONS:

The copyright law of the United States (title 17, U.S. Code) governs the making of photocopies or other reproductions of copyrighted material. Any copying of this document without permission of its author may be prohibited by law.

**Interfacial Fracture Testing in Shape Deposition
Manufacturing**

Nathan W. Kungbeil, J.L. Beuth

EDRC 24-122-95

**Interfacial Fracture Testing in
Shape Deposition
Manufacturing**

**Nathan W. Klingbeil
and
Jack L. Beuth**

Department of Mechanical Engineering and the
Engineering Design Research Center
Carnegie Mellon University
Pittsburgh, PA

This work has been supported by the Engineering Design Research Center,
an NSF Engineering Research Center

ABSTRACT

Shape Deposition Manufacturing (SDM) is a manufacturing process in which three dimensional parts are built up layer by layer, realizing a computer-generated solid model. Because materials are deposited at high temperatures, residual stresses are induced throughout the process. Consequently, there can exist both warping of the part and a tendency to delaminate or fracture between layers, especially between those of dissimilar materials. Thus, in the design of SDM parts, it is important to know the critical energy release rate and mode of crack extension governing interfacial fracture for particular material combinations. Interfacial toughness tests using three layer composite beam specimens under four point bending are examined. Such a test on a two layer specimen has been considered in the literature. A steady-state energy release rate (independent of crack length) is deduced analytically for both the two and three layer specimens. Finite element models verify the analytical predictions and are used to extract the mode of crack extension. Experimental results are obtained for two bimaterial interfaces.

INTRODUCTION

Shape Deposition Manufacturing (SDM) is a manufacturing process which involves the slicing of a computer-generated solid model into layers, followed by the successive deposition and five axis CNC machining of each layer (see Merz, et al., 1994). Because SDM begins with a computer-generated model of the design, it effectively links the design and manufacturing processes. The ultimate goal of SDM is to rapidly create finished parts of any conceivable geometry using real engineering materials. Its applications include manufacturing of embedded electronic components, injection mold tooling, layered metal composites, and parts having complex geometries that cannot be machined by conventional methods.

SDM typically involves layered deposition of molten metals, accomplished by one of two different methods. The first is thermal spray deposition, involving the repeated spraying of molten metal powder. *Parts* manufactured in this manner tend to be porous and brittle, and have low tensile strengths. As a result, a second method (called microcasting) has been developed. Microcasting is a process in which molten metal is dripped onto the substrate. Mechanical properties of microcasted parts are comparable to those of welded metals, and are far superior to those of sprayed parts.

Inherent in the layered deposition of molten metals is the generation of residual stresses. Consequently, SDM parts can exhibit warping and a tendency to delaminate or fracture between layers, particularly between those of dissimilar materials. The focus of this work is to determine critical energy release rates and modes of crack extension governing interfacial fracture for particular material combinations.

These critical parameters are determined using composite beam specimens under four point bending. Such a test for two layer specimens was first considered by Charalambides et al., 1989. Four point bend tests are appropriate for this application for a number of reasons. SDM generated specimens tend to be slightly warped, and are consequently most suitable for bending configurations. In addition, delamination under bending is similar to the actual mode of failure in which free edges tend to bend up, resulting in debonding between layers. Finally, four point bending leads to a steady-state energy release rate (independent of crack length). As a result, it is unnecessary to accurately measure the crack length during fracture, and the experimental procedure is significantly facilitated. In the present work, the two layer test is applied to deposited metal layers. The concept is then generalized to specimens having multiple layers, and is applied to a three layer specimen. Critical fracture parameters are determined for two bimaterial interfaces.

INTERFACIAL FRACTURE MECHANICS

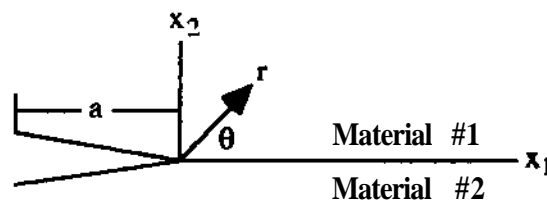


Figure 1. The Interfacial Crack

In order to facilitate a discussion and analysis of interfacial toughness testing, it is first necessary to outline the fundamentals of interfacial fracture mechanics. The mechanics of interface cracking (Figure 1) has been reviewed by Hutchinson and Suo (1991). Interfacial fracture is inherently mixed mode, which means that the crack faces experience both relative opening and sliding displacements. As discussed by Rice (1988) and Suo and Hutchinson (1990), among others, the singular stresses directly ahead of the crack tip (along $G = 0$) take the form

$$\sigma_{22} + i\sigma_{12} = \frac{K r^{1/2}}{\sqrt{27cr}} \quad (1)$$

where $K = K_j + iK_{-j}$ is the complex interface stress intensity factor. Here, Arabic numerals are used to differentiate the interface stress intensity factor from the classical mixed mode stress intensity factor. The parameter ϵ depends on the material property mismatch and is given by

$$\epsilon = \frac{1}{2} \ln \left[\frac{\mu_1 + \mu_2 K_1}{\mu_2 + \mu_1 K_2} \right] \quad (2)$$

where μ_j ($j=1,2$) is the material shear modulus. For plane stress, $K_j = (3 - \nu_j)/(1 + \nu_j)$, while $K_j = 3 - 4\nu_j$ for plane strain. In general, the interface stress intensity factor takes the form

$$K = f \times (\text{applied stress}) \times \sqrt{h}^{1/2} \quad (3)$$

where f is a complex function of the material properties and problem geometry, and h is some characteristic length. In the experiments outlined in this study, the characteristic length is the smaller of the thicknesses of the W_o layers forming the cracked interface. A mode mixity can be described by the phase angle

$$\psi = \tan^{-1} \left(\frac{|\text{Im}(K h^{1/2})|}{\text{Re}(K h^{1/2})} \right) \quad (4)$$

which is defined to be independent of h . The relative crack face displacements are expressed in terms of the interface stress intensity factor as

$$\delta_2 + i\delta_1 = \frac{4(\bar{E}_1 + \bar{E}_2)}{(1 + 2i\epsilon) \cosh(\pi\epsilon)} \sqrt{r} \quad (5)$$

where $\delta_j = U_{j,c}(r,0) - U_{j,c}(r,0 = -ft)$. Here, $E_j = E_j$ for plane stress, while $\bar{E}_j = E_j / (1 - \nu_j^2)$ for plane strain.

The quantity driving crack extension is the energy release rate G , defined as the change in potential energy per unit crack extension and per unit width (B)

$$\frac{1}{B} \frac{dPE}{da}$$

As shown by Malyshev and Salganik (1965), the energy release rate can be expressed in terms of the interface stress intensity factor as

$$G = \frac{K^2}{2 \cosh(\pi\epsilon)} \frac{1}{E^*} \quad (7)$$

The purpose of the current study is to determine the resistance to fracture of particular bimaterial interfaces. This resistance to fracture is a material property, expressed as either the interfacial fracture toughness, K^* , or the critical energy release rate, G_c .

Interfacial fracture mechanics assumes that for a given mode of crack extension and under small scale yielding, crack extension occurs when $|K| = IK^{\wedge}$ (or $G = G_c$) for the interface. It is important to note that fracture mechanics principles are applicable only for small scale yielding; this constraint is seen to have a significant effect on the present work.

SPECIMEN ANALYSIS

The analysis presented in this section does not account for residual stresses in the specimens. These stresses and their contributions to energy release rates may not be small. However, a residual stress model is not currently available to quantify their effects. In the event that accurate residual stress estimates become available, their effects on energy release rates could be easily incorporated into the equations presented and used here.

The Bimaterial Specimen

Abimaterialfour point bend specimen for measuring interfacial fracture toughness has been considered in the literature (Charalambides, et al., 1989). A typical test specimen is depicted in Figure 2.

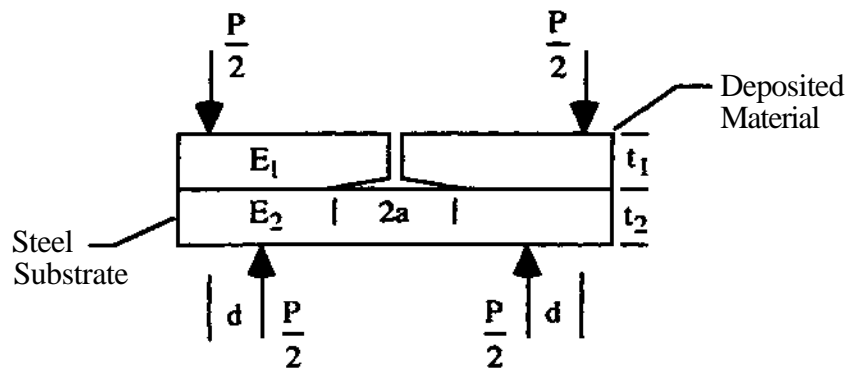


Figure 2. The Bimaterial Specimen

The main advantage of the four point bend specimen is the existence of a steady-state energy release rate for a sufficiently long crack length, $2a$. Between the inner loading points, both the bending moment and the specimen dimensions are constant. The strain energy stored in the composite beam can be determined using elementary beam theory. As a crack extends along the interface, the strain energy is relieved from the debonded portion of the composite beam. Once the crack becomes long enough that the debonded portion

behaves as a stress free beam, the near tip stresses simply translate with the crack front. The change in potential energy as the crack extends is simply the difference in strain energy between corresponding sections of the specimen far ahead of and far behind the crack tip. Thus, the steady-state energy release rate can be deduced analytically as the difference in strain energy between the cracked and uncracked beams, and is given by elementary beam theory as

$$G_{ss} = \frac{M^2}{2E_2 B} \left[\frac{1}{I} - \frac{1}{I_c} \right]. \quad (8)$$

Here, $M = P/2 \cdot d$ is the bending moment, E_2 is the elastic modulus of the bottom layer (the steel substrate), B is the specimen width, and $I = 1/12 B t^3$ is the moment of inertia of the bottom layer alone.

In elementary beam theory, the moment of inertia of a composite beam can be represented as the moment of inertia of an equivalent transformed cross section having the elastic modulus of either of the two materials (see Timoshenko and Gere, 1990, for a detailed explanation). In (8), I_c is the moment of inertia of an equivalent transformed cross section of modulus E_2 , and is given by

$$I_c = B \left[\frac{1}{12} n t^3 + n t_1 (t_2 + t_1/2 - \bar{y})^2 + \frac{1}{12} t_2^3 + t_2 (t_2/2 - \bar{y})^2 \right], \quad (9)$$

where $n = E_j/E_2$. The quantity \bar{y} represents the location of the neutral axis of the composite beam measured from the bottom of the steel substrate, and is given by

$$\bar{y} = \frac{t_2^2 + 2 n t_1 t_2}{2(n t_1 + t_2)}. \quad (10)$$

It is important to note that in addition to an explicit dependence on E_2 , G_{ss} has an implicit dependence on the modulus of the deposited layer (through n).

Finite element results for the steady-state energy release rates and phase angles of bimaterial specimens are provided in the literature over a wide range of material combinations (Charalambides, et al., 1989). These results are used to verify the analytical prediction for G_{ss} , as well as to determine the mode mixity. The procedure for extracting the phase angle from numerical results is outlined in the section describing the three layer specimen.

As previously mentioned, critical fracture parameters can only be determined under small scale yielding. Consequently, specimen dimensions must be designed such that large scale yielding of the bottom beam does not occur prior to crack extension. The bending moment required for crack extension is found by setting $G_{ss} = G_c$ and inverting equation (8), and is given as

$$M_{\text{ext}} = \frac{2E_2 I B G_c I_c}{I_c - I} \quad (11)$$

The moment required to yield the bottom beam is simply

$$M_y = \frac{2\sigma_y l}{t} \quad (12)$$

where σ_y is the yield stress of the bottom beam. The condition for fracture prior to yielding of the lower beam is

$$\frac{M_{\text{ext}}}{M_y} < 1. \quad (13)$$

The above condition can be satisfied for any given G_c by using layers of equal thickness, $t_1 = t_2 = t$, and increasing the total thickness, $2t$ (see Charalambides, et al., 1989). An inherent problem with specimen design is that proper dimensions can only be ensured if G_c is **known a priori**, which is obviously not the case. Thus, an educated guess regarding the fracture toughness of an interface must be made prior to specimen design.

The Three Layer Specimen

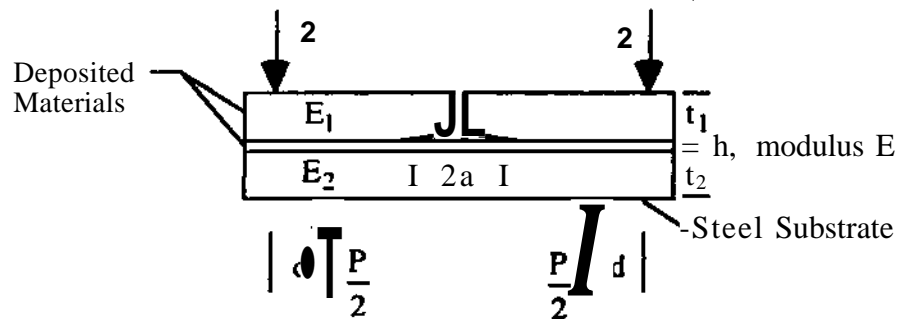


Figure 3. The Three Layer Specimen

The bimaterial specimen is useful for determining the interfacial toughness between a deposited layer and a substrate. In order to obtain the toughness between two deposited materials, a specimen having at least three layers is required. For two layer specimens, suitable dimensions can be obtained using layers of equal thickness. Such dimensions are approximated for three layer specimens by using a thin middle layer of thickness h , and having top and bottom layers of roughly equal thickness, as shown in Figure 3.

The analytical deduction of G_{ss} is analogous to that for the two layer problem, and can also be obtained by applying elementary beam theory. Here, the steady-state energy release rate becomes

$$G_{ss} = \frac{M^2}{2E_2BLI_c} \left[\frac{1}{I_c} - \frac{1}{I_{c3}} \right], \quad (14)$$

where I_c corresponds to the composite beam beneath the crack, and I_{c3} corresponds to the three layer composite beam.

Both I_c and I_{c3} are obtained by considering transformed cross sections of elastic modulus E_2 . Using the previous definition for n , and defining $n_2 = E/E_2$, where E is the modulus of the thin middle layer, the moment of inertia of the three layer composite beam is

$$I_{c3} = B \left[\frac{1}{12} n t^3 + n t \left(\frac{t_0 + h + t}{2} - \bar{y} \right)^2 + \frac{1}{12} n_2 h^3 + n_2 h \left(t_2 + \frac{h}{2} - \bar{y} \right)^2 + \frac{1}{12} t_2^3 + t_2 \left(\frac{t_2}{2} - \bar{y} \right)^2 \right], \quad (15)$$

Here, the location of the neutral axis is given as

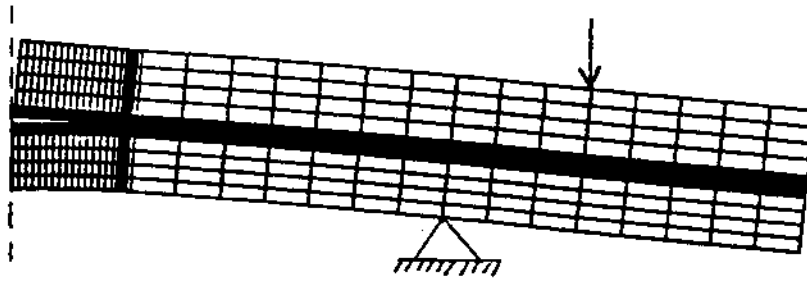
$$\bar{y} = \frac{2nt(t_2 + h) + nt^2 + 2n_2t_2h + n_2h^2 + t_2^2}{2(ntj + nh + t)}. \quad (16)$$

I_c can be obtained by setting $I_{c3} = I_c$ and evaluating equations (15) and (16) for $l = 0$.

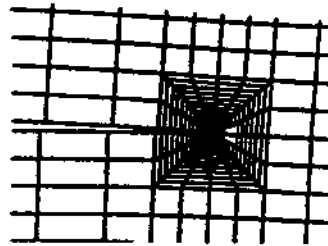
The equations presented here do not require h to be small compared to t and t_2 , as depicted in Figure 3. As h approaches zero, however, the solution for G_{ss} obtained for the two layer beam is recovered. Note that the approach applied here for three layer specimens is quite general, and can be used for specimens having any number of layers.

In order to verify the analytical prediction of G_{ss} and to determine its region of applicability, as well as to extract the mode of crack extension, a finite element model of the three layer specimen has been constructed using the software package ABAQUS. The numerical results presented here are for the microcasted specimen discussed in the next section, but the procedure is quite general. The model has a middle layer of thickness h , and top and bottom layers each of thickness $6h$. For the far-field region, the model uses eight-noded plane stress quadrilateral interpolation elements. A refined mesh of quarter-point elements is used near the crack tip to capture the $1/\sqrt{r}$ singularity. The near-tip mesh consists of 18 rings of elements meshed over a length of $h/2$. Because the problem is symmetric about the midplane, only half the specimen is modeled. The deformed far-field and near-tip meshes are shown in Figure 4. The near-tip mesh (Figure 4b) clearly illustrates the relative opening and sliding crack face displacements that are indicative of mixed mode loading.

The energy release rate G has been directly determined from a J integral for a number of crack lengths. The normalized energy release rate, G/G_{ss} , is plotted in Figure 5



a) The Deformed Specimen



b) The Near-Tip Region

Figure 4. The Deformed Finite Element Mesh

as a function of the normalized crack length, a/h ; The energy release rate is seen to approach steady-state for crack lengths of $a/h \ll 5$, which is on the order of the thickness of the debonded portion of the beam. Thus, it is for cracks of this length that the debonded portion begins to act like a stress free beam, and the change in strain energy as the crack extends is just the difference in strain energy between the cracked and uncracked beams.

In addition to verifying the analytical prediction for G_{ss} , the numerical results are used to determine the mode mixity (designated by ψ in equation (4)). The procedure used is outlined by Mates, et al., 1989. By inverting equation (5), the interface stress intensity factor is determined in terms of the relative crack face displacements as

$$K = \left(\frac{(1 + 2i\epsilon) \cosh(\pi\epsilon) \bar{E}_1 \bar{E}_2}{4(\bar{E}_1 + \bar{E}_2)} \right) \left(\frac{2\pi}{r} \right)^{1/2} r^{-i\epsilon} (\delta_2 + i\delta_1). \quad (17)$$

At each node point located at a distance r behind the crack tip, the relative crack face displacements are extracted from the finite element solution, and the complex stress intensity factor is computed using equation (17). The energy release rate is then calculated

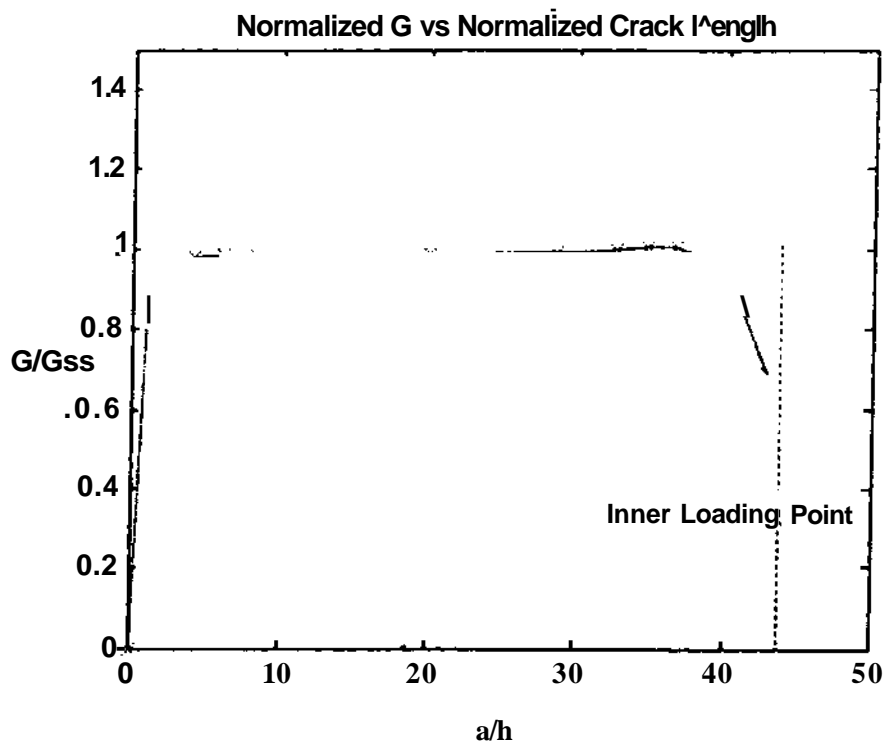


Figure 5. Normalized G vs. Crack Length

using equation (7). and compared to independent contour integral estimates. The phase angle, ψ , is evaluated using equation (4) at the distance r where the interface mechanics solution most closely matches the contour integral estimates, which typically occurs within the second or third element from the crack tip at a distance on the order of $h/100$. In accordance with the finite element model, evaluations of (7) and (17) are carried out for the case of plane stress.

EXPERIMENTAL PROCEDURE AND RESULTS

Sprayed Specimens

The bimaterial specimen was used in this work to determine the fracture toughness of a nickel-aluminum (4% Al) powder sprayed on a carbon steel substrate. Because the spraying process yields a porous and partially oxidized deposit, the material properties are not easily predicted. As a result, it was first necessary to determine the material properties

of the deposited layer experimentally. The test configuration is shown in Figure 6. The strains on the top and bottom of an uncracked bimaterial specimen in four point bending

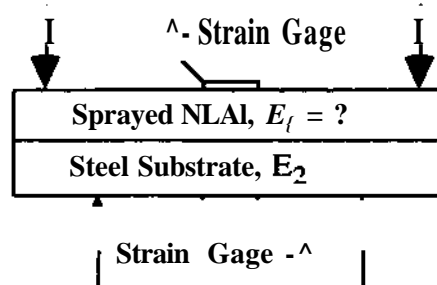


Figure 6. Determination of Sprayed Material Properties

were measured simultaneously. Elementary beam theory was then used to determine the ratio of the elastic moduli of the top and bottom layers that was required to produce the measured strains. Since the modulus of the steel plate used for the substrate was known from an independent test ($E_2 = 27.5 \times 10^4$ psi), the modulus of the sprayed layer was easily determined. The presence of two strain gages also allowed for a direct calculation of E_1 , which was used as a check against the independently measured value. The Poisson's ratio of the sprayed material was taken directly from the strain gage measurements. For sprayed NiAl, the material properties measured were $E_1 = 9.9 \times 10^4$ psi and $\nu_1 = 0.19$.

Once the material properties of the bimaterial specimen were known, it was possible to use the equations presented in the previous section in determining the interfacial fracture parameters. The test configuration was that shown in Figure 2. The deposited NiAl layer had thickness $t_1 = 0.076$ ", and the thickness of the steel substrate was $t_2 = 0.059$ ". Specimens were cut to widths $B = 0.75$ " and lengths equal to 6". The moment arm used during testing was $d = 0.5$ ".

Prior to actual testing, the specimen was loaded and unloaded two or three times so that a steady-state crack extended from the notch. This was done to avoid erratic crack propagation due to initial debonding. Loading was then slowly applied at constant displacement rate. The analytical solution for G_{ss} suggested that for constant interfacial toughness, steady-state fracture would occur at constant load. A typical plot of load vs. time for a sprayed NiAl specimen is given in Figure 6. Because the loading was applied at constant displacement rate, load vs. time corresponds to load vs. displacement. The specimen was initially loaded to $P = 15$ lbs in order to stabilize it in the bending fixture. Test results show the load initially increasing linearly with displacement. Once the critical load was reached, it remained constant throughout crack propagation. The critical

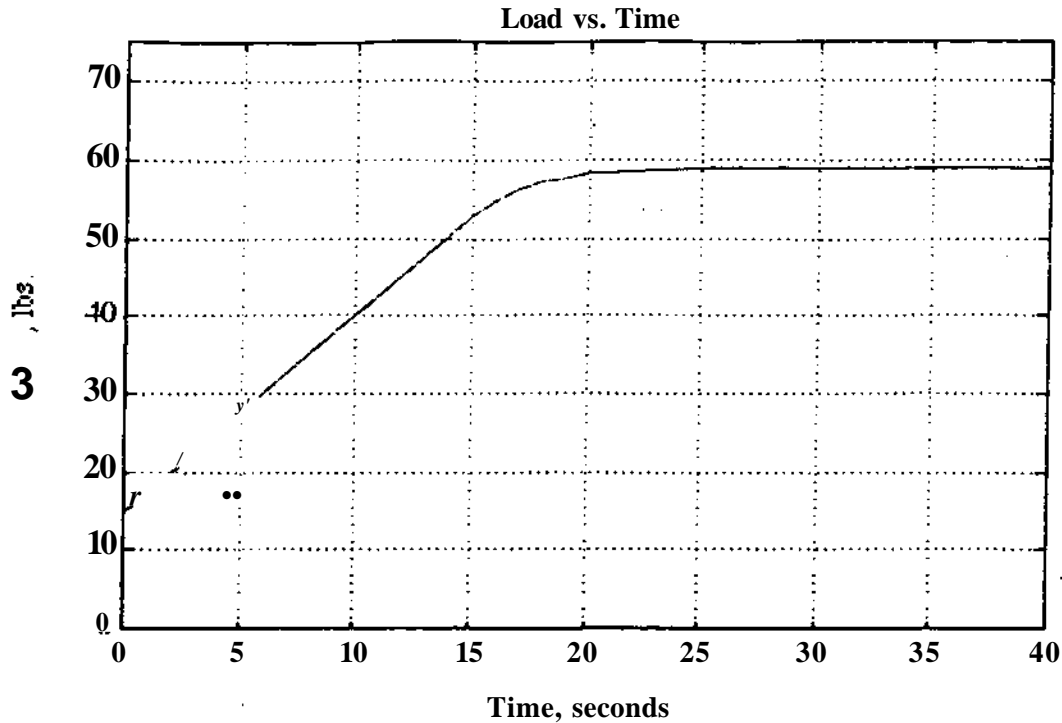


Figure 6. Load vs. Time for NiAl Sprayed on Carbon Steel

energy release rate was calculated by setting $G = G_c$ and evaluating equation (8) at the bending moment at which fracture occurred. The interfacial fracture toughness, IK^{\wedge} , was related to G_c through equation (7). Since plane strain conditions prevail near the crack tip, the plane strain form of (7) was used here. A phase angle of $Xf \sim 45^{\circ}$ was specified from the finite element results for bimaterial specimens presented in the literature (Charalambides, et al 1989).

Similar tests were conducted on three additional specimens, and a summary of the results is given in Table 1. The plot in Figure 6 was obtained for Specimen #1. Average values of the critical parameters calculated for NiAl sprayed on carbon steel, for $\|f = 45^{\circ}$, are $G_c = 0.30 \text{ lb/in}$ and $(K^{\wedge} 2.2 \times 10^3 \text{ psi}\sqrt{\text{in}})$.

Table 1. Critical Interfacial Fracture Parameters for NiAl Sprayed on Carbon Steel Under Mixed Mode Loading of $\|f = 45^{\circ}$

Specimen #	$G_c, \text{ lb/in}$	$IK^{\wedge}, \text{ psU/iit}$
1	0.28	2.1×10^3
2	0.36	2.4×10^3
3	0.21	1.9×10^3
4	0.35	2.4×10^3

Microcasted Specimens

In the transition from thermal spraying to microcasting, the problem of debonding between layers of identical material has been substantially reduced. In deposition of stainless steel, for example, an interface between layers is often difficult to distinguish. Delamination in microcasted parts is most prevalent between dissimilar materials. Microcasted parts are commonly manufactured using both stainless steel and copper. Copper is used as a sacrificial support material, which provides structure for the stainless steel part during the manufacturing process and is later chemically etched away. In addition, copper can be used in conjunction with stainless steel to produce multi-material parts. Thus, it is of interest to determine the toughness of interfaces between these materials, and a number of specimens were designed to this end. Specimens included copper dripped on stainless steel, copper dripped on copper, and stainless steel dripped on copper. In general, the bonding between microcasted layers was better than had been anticipated. It was difficult to achieve fracture prior to yielding of the lower beam, despite the use of specimen dimensions much larger than those used for the sprayed NiAl. Fracture parameters were determined, however, for two specimens consisting of stainless steel dripped on copper.

As shown in Figure 7, the specimens were inverted from the manufactured

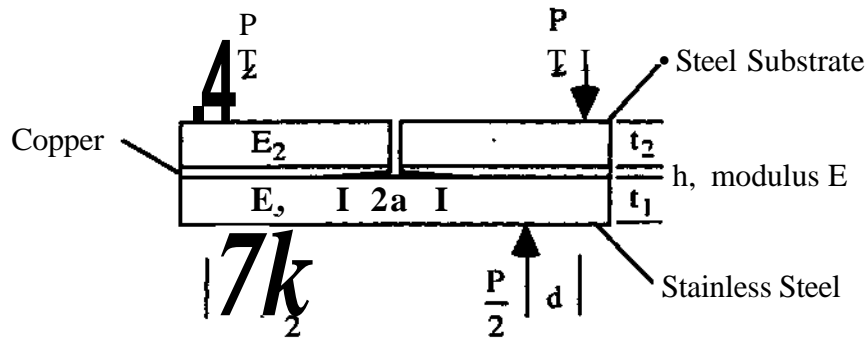


Figure 7. Three Layer Specimen for Stainless Steel Dripped on Copper

configuration during testing. This was done in order to avoid yielding of the copper layer prior to crack extension. The copper layer would be likely to yield if it were to remain in the lower portion of the partially debonded beam, because it has a much lower yield point than stainless steel and would be located at the furthest possible point from the neutral axis. Layer thicknesses were $t_j = t_2 = 0.240$ " and $h = 0.040$ ". Specimens were cut to widths

of $B = 0.75''$ and lengths equal to $5''$. As in the tests on sprayed specimens, the moment arm used was $d = 0.5''$

The first specimen was tested using a procedure similar to that used for the sprayed specimens. An initial crack was introduced by loading and unloading the specimen two or three times. The specimen was then slowly loaded at constant displacement rate. In contrast to the fracture observed for the sprayed specimens, the crack did not propagate at constant load. Evidently, the toughness of the interface was not constant. Critical energy release rates were calculated by setting $G = G_c$ and evaluating equation (14) at each value of the bending moment at which the crack extended. Note that the evaluation of I_{c3} is not affected by the inverted specimen configuration. I_c is calculated by setting $I_{c3} = I_c$ and evaluating equations (15) and (16) for $t_0 = h = 0$. Interfacial toughnesses were related to the critical energy release rates by using equation (7) and assuming plane strain near the crack tip. A number of G_c and (K^I) values were calculated at various crack lengths for the same interface, and are listed in order of increasing crack lengths in Table 2. In the final configuration ($a = 0.40$ in) no crack growth was possible before yielding of the stainless steel. A phase angle of $\psi = 42^\circ$ was extracted from finite element results for this specimen configuration in the manner previously described. As seen from the table, the

Table 2. Critical Interfacial Fracture Parameters for Stainless Steel Drilled on Copper Under Mixed Mode Loading of $\psi = 42^\circ$, Specimen #1

G_c , lb/in	$JKI_{I,II}$, psi \sqrt{in}
0.52	3.6×10^3
0.71	4.3×10^3
1.2	5.5×10^3
4.2	1.0×10^4

toughness for this first specimen increased with crack length, but this result was not likely related to an R-curve effect. Instead, variations in toughness likely resulted randomly from variances in the bonding conditions inherent in the microcasting process.

Critical fracture parameters were also determined for a second specimen, but the procedure was slightly different. Once again, an initial crack was introduced and monotonic loading was applied until the crack extended. The crack length and critical load at crack extension were recorded. Monotonic loading was then resumed, but the crack would not propagate further prior to yielding of the lower beam. In order to get past this

region of higher toughness, the specimen was fatigued below the yield point until the crack extended, at which time monotonic loading was reapplied. This procedure was repeated, and a total of three toughnesses were recorded at different crack lengths. Fatigue was typically performed using an inverted haversine signal at a frequency of 10 Hz, for a period of twenty minutes. Maximum and minimum loads were 1400 lb and 800 lb, respectively (yielding of the specimen was expected at 2000 lb). These loads corresponded to a variance in the stress intensity factor of $A|K| = 1800 \text{ psi}\sqrt{\text{in}}$ at a mean value of $|K|_m = 8500 \text{ psi}\sqrt{\text{in}}$. The critical parameters and corresponding crack lengths calculated for this specimen are given in Table 3.

Table 3. Critical Parameters and Crack Lengths for Stainless Steel Drilled on Copper Under Mixed Mode Loading of $\psi = 42^\circ$, Specimen #2

2a, in	G_c , lb/in	IK^\wedge , psh/ $\sqrt{\text{in}}$
0.383	3.7	9.7×10^3
0.908	1.5	6.1×10^3
1.07	3.7	9.7×10^3

As seen from the data recorded for each specimen, the toughness of microcasted interfaces can vary considerably. Using data from both specimens, average critical parameters calculated for stainless steel drilled on copper, for $\psi = 42^\circ$, are $G_c = 2.2 \text{ lb/in}$ and $|K|_m = 7.5 \times 10^4 \text{ psi}\sqrt{\text{in}}$. As a point of comparison, the pure mode I toughness of steel is typically between 50×10^4 and $200 \times 10^4 \text{ psi}\sqrt{\text{in}}$, depending on the type of steel. Although the toughnesses calculated here were relatively low, they were determined at the weakest points in the interface; the toughnesses at crack lengths for which fracture prior to yielding was not possible were likely much higher. It is clear that microcasting has significantly increased the interfacial toughnesses of SDM parts. Even the relatively brittle stainless steel / copper interface studied here had an average toughness of over three times that of NiAl sprayed on carbon steel.

SUMMARY AND CONCLUSIONS

A test method for determining the fracture toughness of bimaterial interfaces was extended to three layer specimens and used to determine interfacial toughnesses of parts manufactured by SDM. Critical fracture parameters were determined for NiAl sprayed on

carbon steel, as well as for stainless steel dripped on copper. The four point bend test proved useful for interfaces having relatively low toughness, although fracture prior to yielding was difficult to obtain for some higher toughness interfaces.

The transition to microcasting has clearly increased the interfacial toughnesses of SDM parts. Interfacial fracture is not a major concern for stainless steel dripped on stainless steel, for which an interface is barely discernible. Interfacial debonding was not possible prior to yielding for specimens consisting of copper dripped on copper and copper dripped on stainless steel. The most brittle interface tested was stainless steel dripped on copper, for which the average toughness was over three times that of NiAl sprayed on carbon steel. The toughness of each microcasted specimen, however, was seen to vary significantly along the interface. Because no debonding is desired, this result could have substantial implications for how microcasted parts are designed and manufactured.

ACKNOWLEDGMENTS

The authors gratefully acknowledge the support of the National Science Foundation graduate Research Traineeship Program, Grant No. EEC-9256665, the Carnegie Mellon University Department of Mechanical Engineering and the Engineering Design Research Center, an Engineering Research Center of the National Science Foundation, under Grant No. EEC-8943164. The authors would like to thank John Zinn for his assistance during interfacial fracture testing, and John Carbone for his testing to determine the elastic properties of sprayed NiAl, and also Lee Weiss and Fritz Prinz for their thoughts and insights related to this research.

REFERENCES

- Beuth, J.L., and Narayan, S.H., 1995, "Residual Stress-Driven Delamination in Shape Deposited Materials," To be published in the *International Journal of Solids and Structures*.
- Charalambides, P.G., Lund, J., Evans, A.G., and McMeeking, R.M., 1989, "A Test Specimen for Determining the Fracture Resistance of Bimaterial Interfaces," *Journal of Applied Mechanics*, Vol. 56, pp. 77-82.
- Hutchinson, J.W., and Suo, Z., 1991, "Mixed Mode Cracking in Layered Materials," *Advances in Applied Mechanics*, Vol. 28. (Edited by J.W. Hutchinson and T.Y. Wu), Academic Press.
- Malyshev, B.M. and Salganik, R.L., 1965, "The Strength of Adhesive Joints Using the Theory of Cracks," *International Journal of Fracture Mechanics*, Vol. 5, pp. 114-128.

- Matos, P.P.L., McMeeking, R.M., Charalambides, P.G., and Drory, M.D., 1989, "A Method for Calculating Stress Intensities in Bimaterial Fracture," *International Journal of Fracture*, Vol. 40, pp. 235-254.
- Merz, R., Prinz, F.B., Ramaswami, K., Terk, M. and Weiss, L.E., 1994, "Shape Deposition Manufacturing," Proc. Solid Freeform Fabrication Symposium, H. Marcus, J.J. Beaman, J.W. Barlow, K.L. Bourell and R.H. Crawford eds., The University of Texas at Austin, August, pp. 1-8.
- Rice, J.R., 1988, "Elastic Fracture Mechanics Concepts for Interfacial Cracks," *Journal of Applied Mechanics*, Vol. 55, pp. 98-103.
- Suo, Z. and Hutchinson, J.W., 1990, "Interface Crack Between Two Elastic Layers," *International Journal of Fracture*, Vol. 43, pp. 1-18.
- Timoshenko, S. and James M. Gere, Mechanics of Materials, 3d ed. Boston: PWS-KENT Publishing Company, 1990.